Cleavage of $Ru_3(CO)_{12}$ by N-Heterocyclic Carbenes: Isolation of *cis*- and *trans*-$Ru(NHC)_2(CO)_3$ and Reaction with O_2 To Form $Ru(NHC)_2(CO)_2(CO_3)$

Charles E. Ellul,[†] Olly Saker,[†] Mary F. Mahon,[†] David C. Apperley,[‡] and Michael K. Whittlesey*,[†]

Department of Chemistry, University of Bath, Claverton Down, Bath BA2 7AY, U.K., and Department of Chemistry, Durham University, South Road, Durham DH1 3LE, U.K.

Received September 13, 2007

The N-heterocyclic carbenes (NHCs) 1,3-dialkyl-4,5-dimethylimidazol-2-ylidene (alkyl = ethyl, IEt_2Me_2; isopropyl, $I^iPr_2Me_2$) and 1,3-di-isopropylimidazol-2-ylidene (I^iPr_2) cleave $Ru_3(CO)_{12}$ at room temperature to give the mononuclear complexes $Ru(NHC)_2(CO)_3$ (NHC = IEt_2Me_2 **1**; $I^iPr_2Me_2$ **2**; I^iPr_2, **3**). X-ray crystallography reveals that **1** contains *trans*-NHC ligands whereas **2** and **3** have an unexpected cis arrangement of carbenes. Exposure of **1**−**3** to air in the solid state or upon reaction with O_2 in solution yields the carbonato complexes $Ru(NHC)_2(CO)_2(CO_3)$ (NHC = IEt_2Me_2 **4**, $I^iPr_2Me_2$ **5**, I^iPr_2, **6**).

Introduction

Historically, there has been a long-standing connection between N-heterocyclic carbene (NHC) ligands and metal–carbonyl complexes. One of the first examples of a transition-metal NHC complex was $Cr(IMe_2)(CO)_5$ (IMe_2 = 1,3-dimethylimidazol-2-ylidene), which was reported by Öfele as long ago as 1968.[1] About a decade later, Lappert and co-workers showed that highly reactive M(0) carbonyl complexes, such as $Fe(CO)_5$, could break the C=C bond in enetetramines (or carbene "dimers") to afford the mono- and disubstituted carbene complexes $Fe(NHC)(CO)_4$ and $Fe(NHC)_2(CO)_3$.[2] The ruthenium analogues were not described, presumably due to the difficulties associated with working with $Ru(CO)_5$. The more stable Ru-CO precursor $Ru_3(CO)_{12}$ gave the monosubstituted trimer $Ru_3(CO)_{11}(NHC)$ upon breaking the enetetramine C=C bond at elevated temperature.[2] Since this latter report, there have been relatively few examples detailing the reactions of metal–carbonyl dimers[3] or trimers with NHCs.[4,5] In one recent example, Cabeza and co-workers showed that as in Lappert's work, a single CO ligand in $Ru_3(CO)_{12}$ could be displaced at room temperature by IMe_2 to produce $Ru_3(CO)_{11}(IMe_2)$. Subsequent heating at 70 °C in THF led to a remarkable double C−H bond activation of one of the *N*-Me substituents as shown in Scheme 1. The C−H cleavage could be reversed by addition of 1 atm of CO.[4]

Scheme 1

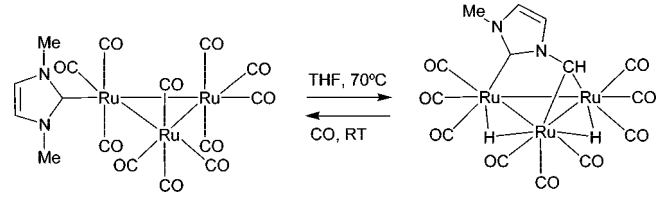

Scheme 2

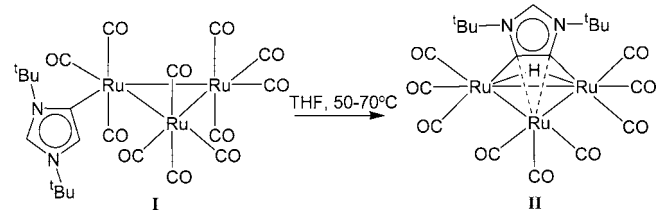

Intrigued by this report, we set out to investigate the reactivity of $Ru_3(CO)_{12}$ with a range of other *N*-alkyl-substituted NHCs. In the case of the very bulky carbene 1,3-di-*tert*-butylimidazol-2-ylidene (I^tBu), coordination takes place though one of the backbone C4/C5 positions to give the "abnormal" carbene complex **I** (Scheme 2) at room temperature. It is likely that the steric bulk of the two *tert*-butyl groups blocks coordination of the NHC at the "normal" C2 position.[6] Upon heating **I**, activation of the remaining backbone C−H bond takes place to give a new product **II**, in which the carbene bridges two ruthenium atoms while at the same time interacting with the third in a Ru_3C_2 5c−4e bonding interaction. The formation of this bridging heterocycle via a double "abnormal" interaction represents a new binding motif in NHC chemistry and suggests

* To whom correspondence should be addressed. E-mail: chsmkw@bath.ac.uk.
[†] University of Bath.
[‡] Durham University.

(1) Öfele, K. *J. Organomet. Chem.* **1968**, *12*, P42–P43.

(2) Lappert, M. F.; Pye, P. L. *J. Chem. Soc., Dalton Trans.* **1977**, 2172–2180.

(3) (a) Carty, A. J.; Taylor, N. J.; Smith, W. F.; Lappert, M. F.; Pye, P. L. *J. Chem. Soc., Chem. Commun.* **1978**, 1017–1019. (b) Herrmann, W. A.; Elison, M.; Fischer, J.; Köcher, C.; Artus, G. R. J. *Chem. Eur. J.* **1996**, *2*, 772–780. (c) Gibson, S. E.; Johnstone, C.; Loch, J. A.; Steed, J. W.; Stevenazzi, A. *Organometallics* **2003**, *22*, 5374–5377. (d) van Rensburg, H.; Tooze, R. P.; Foster, D. F.; Slawin, A. M. Z. *Inorg. Chem.* **2004**, *43*, 2468–2470. (e) Tye, J. W.; Lee, J.; Wang, H.-W.; Mejia-Rodriguez, R.; Reibenspies, J. H.; Hall, M. B.; Darensbourg, M. Y. *Inorg. Chem.* **2005**, *44*, 5550–5552. (f) Capon, J.-F.; El Hassnaoui, S.; Gloaguen, F.; Schollhammer, P.; Talarmin, J. *Organometallics* **2005**, *24*, 2020–2022. (g) van Rensburg, H.; Tooze, R. P.; Foster, D. F.; Otto, S. *Inorg. Chem.* **2007**, *46*, 1963–1965. (h) Morvan, D.; Capon, J.-F.; Gloaguen, F.; Le Goff, A.; Marchivie, M.; Michaud, F.; Schollhammer, P.; Talarmin, J.; Yaouanc, J.-J.; Pichon, R.; Kervarec, N. *Organometallics* **2007**, *26*, 2042–2052.

(4) Cabeza, J. A.; del Río, I; Miguel, D.; Sánchez-Vega, M. G. *Chem. Commun.* **2005**, 3956–3958.

(5) Cooke, C. E.; Ramnial, T.; Jennings, M. C.; Pomeroy, R. K.; Clyburne, J. A. C. *Dalton Trans.* **2007**, 1755–1758.

(6) Ellul, C. E.; Mahon, M. F.; Saker, O.; Whittlesey, M. K. *Angew. Chem., Int. Ed.* **2007**, *46*, 6343–6345.

10.1021/om700915t CCC: $40.75
Publication on Web 12/15/2007

Scheme 3

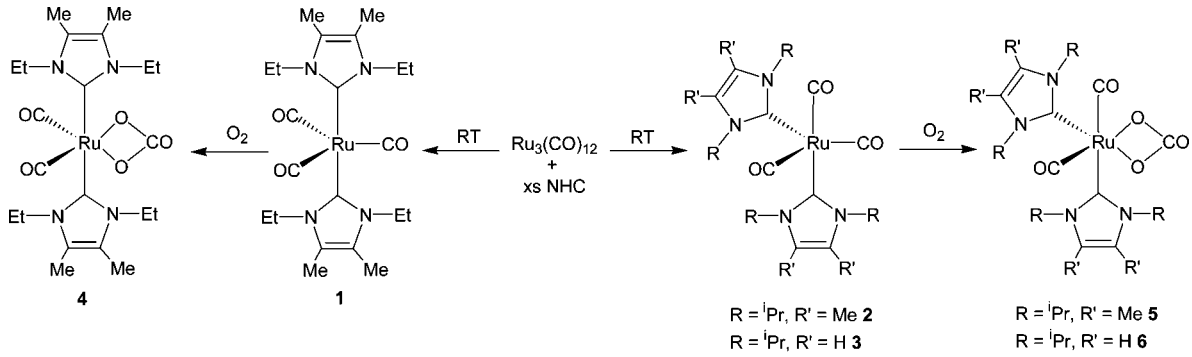

that other, unusual patterns of carbene reactivity might be available with metal cluster precursors.

We now report that in the presence of excess *N*-Et or *N*-^{i}Pr carbenes, $Ru_3(CO)_{12}$ is broken up at room temperature to give the mononuclear tricarbonyl complexes $Ru(NHC)_2(CO)_3$ in good yields, with no formation of cluster products comparable to **I** or **II**.[7,8] Contrary to the many well-known examples of trigonal bipyramidal (tbp) $Ru(PR_3)_2(CO)_3$ species which contain trans-donor ligands[9] (which are favored on electronic grounds[10]), the molecular structures of the two *N*-^{i}Pr complexes $Ru(I^iPr_2Me_2)_2(CO)_3$ (**2**, $I^iPr_2Me_2$ = 1,3-diisopropyl-4,5-dimethylimidazol-2-ylidene) and $Ru(I^iPr_2)_2(CO)_3$ (**3**, I^iPr_2 = 1,3-diisopropylimidazol-2-ylidene) contain cis NHC ligands. In contrast, **1**, which contains the less bulky IEt_2Me_2 (1,3-diethyl-4,5-dimethylimidazol-2-ylidene) ligand, displays a tbp structure with trans carbenes. All three complexes prove susceptible to oxidation in solution and in the solid state to give the dicarbonyl carbonato complexes $Ru(NHC)_2(CO)_2(CO_3)$.

Results and Discussion

Reaction of $Ru_3(CO)_{12}$ with IEt_2Me_2. The addition of 6 equiv of IEt_2Me_2 to a THF solution of $Ru_3(CO)_{12}$ resulted in the rapid, room-temperature evolution of CO and formation of $Ru(IEt_2Me_2)_2(CO)_3$ (**1**), which was isolated as an orange-red solid in 83% yield (Scheme 3). The simplicity of the ^{13}C NMR spectrum of **1** in THF-d_8 (solution NMR data are discussed further below), which contained just two high-frequency resonances at δ 181.6 and 218.6, assigned to N*C*N and Ru*C*O, respectively, implies a trans-axial NHC arrangement as found previously in both $Ru(IMes)_2(CO)_3$ and $Ru(ICy)_2(CO)_3$ (IMes = 1,3-bis(2,4,6-trimethylphenyl)imidazol-2-ylidene; ICy = 1,3-dicyclohexylimidazol-2-ylidene).[11,12] Confirmation of the trans-NHC stereochemistry in **1** was provided by X-ray crystallography, as shown in Figure 1. The molecular structure consists of a distorted trigonal bipyramid with a C_{NHC}−Ru−C_{NHC} angle of 172.24(9)° (Table 1). One of the OC−Ru−CO angles is considerably more acute than either of the other two (C(1)−Ru−C(2), 103.64(14); C(1)−Ru−C(3), 124.34(13); C(2)−Ru−C(3), 131.98(13)°), a feature also noted in the mixed carbene phosphine complex $Ru(IMes)(PPh_3)(CO)_3$.[13] The widening of the latter two angles from the idealized value of 120° coincides with tilting of the NHC ligands toward the enlarged equatorial gaps (N(3)−C(13)−Ru(1), 131.11(17); N(4)−C(13)−Ru(1), 126.09(17); N(1)−C(4)−Ru(1), 127.01(17); C(6)−C(5)−N(1), 106.1(2)°). These tilts are further evidenced by the proximity of one methylene hydrogen of an *N*-Et group to the ruthenium center, relative to the corresponding hydrogen on the opposite ethyl group of the ligand (H(20B)···Ru(1), 2.99; H(16A)···Ru(1), 3.23; H(7A)···Ru(1), 3.01; H(11A)···Ru(1), 3.13 Å). Also notable is the relative twist of the axial NHC ligands with an angle of 46.1° between the least-squares NHC ring planes.

Differences in the carbonyl ligands were also apparent from the solid-state ^{13}C NMR spectrum of **1**. Spectra recorded at 303 and 206 K showed three distinct CO signals at δ 224, 214, and 212. At 303 K, the Ru−C_{NHC} resonance consisted of two, just-resolved, lines at δ 177.3 and 177.9, but at 206 K, the resonance consisted of a single, broader line at δ 176.8. Further evidence for ligand asymmetry, this time in the orientation of the carbene ligands, was illustrated by the appearance of eight different methyl resonances (these were most clearly separated at low temperature as evident in Figure 2), as well as four ^{15}N signals (Figure 2).

Reaction of $Ru_3(CO)_{12}$ with $I^iPr_2Me_2$ and I^iPr_2. $Ru_3(CO)_{12}$ also reacted vigorously at room temperature with 6 equiv of $I^iPr_2Me_2$ and I^iPr_2 to give **2** and **3** (Scheme 3).[14,15] In both cases, X-ray crystallography revealed an unexpected cis-arrangement of the two carbene ligands (Figure 3) with C_{NHC}−Ru−C_{NHC} angles of 88.52(7)° and 87.55(8)° for **2** and **3**, respectively (Table 1). The axial Ru−NHC bond lengths (**2**, 2.178(2) Å; **3**, 2.153(2) Å) are considerably shorter than the equatorial distances (2.2019(17); 2.177(2) Å) and in all cases longer than those found

(7) Formation of an analogous N-heterocyclic silylene complex $Ru(NHSi)_2(CO)_3$ from $Ru_3(CO)_{12}$ has been described: Schmedake, T. A.; Haaf, M.; Paradise, B. J.; Millevolte, A. J.; Powell, D. R.; West, R. *J. Organomet. Chem.* **2001**, *636*, 17–25.

(8) Although $Ru_3(CO)_{12}$ is well-known to fragment upon reaction with tertiary phosphines, forcing conditions involving heat (Pöe, A.; Twigg, M. V. *Inorg. Chem.* **1974**, *13*, 2982–2985) or photolysis (Johnson, B. F. G.; Lewis, J.; Twigg, M. V. *J. Organomet. Chem.* **1974**, *67*, C75−C76) are required and invariably lead to mixtures of $Ru(PR_3)_x(CO)_y$ (x = 1, y = 4; x = 2, y = 3).

(9) (a) Collman, J. P.; Roper, W. R. *J. Am. Chem. Soc.* **1968**, *87*, 4008–4009. (b) Jones, R. A.; Wilkinson, G.; Galas, A. M. R.; Hursthouse, M. B.; Abdul Malik, K. M. *J. Chem. Soc., Dalton Trans.* **1980**, 1771–1778. (c) Espuelas, J.; Esteruelas, M. A.; Lahoz, F. J.; Lopez, A. M.; Oro, L. A.; Valero, C. *J. Organomet. Chem.* **1994**, *468*, 223–228. (d) Bodensieck, U.; Vahrenkamp, H.; Rheinwald, G.; Stoeckli-Evans, H. *J. Organomet. Chem.* **1995**, *488*, 85–90. (e) Heyn, R. H.; Macgregor, S. A.; Nadasdi, T. T.; Ogasawara, M.; Eisenstein, O.; Caulton, K. G. *Inorg. Chim. Acta* **1997**, *259*, 5–26.

(10) Rossi, A. R.; Hoffmann, R. *Inorg. Chem.* **1975**, *14*, 365–374.

(11) Jazzar, R. F. R.; Bhatia, P. H.; Mahon, M. F.; Whittlesey, M. K. *Organometallics* **2003**, *22*, 670–683.

(12) Burling, S.; Kociok-Köhn, G.; Mahon, M. F.; Whittlesey, M. K.; Williams, J. M. J. *Organometallics* **2005**, *24*, 5868–5878.

(13) Abdur-Rashid, K.; Fedorkiw, T.; Lough, A. J.; Morris, R. H. *Organometallics* **2004**, *23*, 86–94.

(14) The use of <6 equiv of carbene was investigated for the reaction with $I^iPr_2Me_2$. It was found that while complex **2** was formed, two other uncharacterized products were also produced.

(15) Signals for complex **2** can also been seen upon thermolysis of $Ru(PPh_3)_2(CO)_3$ in the presence of excess $I^iPr_2Me_2$ at 333 K, showing that the *cis*-NHC arrangement is not simply a kinetic phenomenon. However, the reaction is slow and leads to a number of other unidentifiable products being formed (see ref 19).

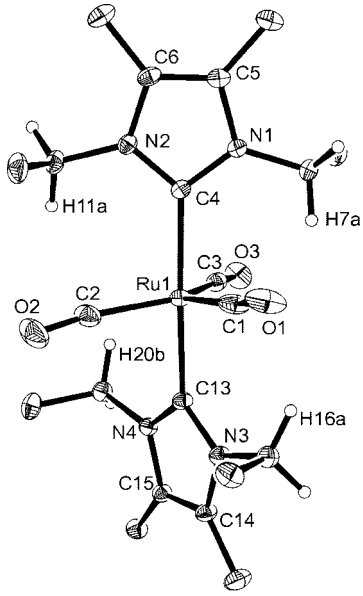

Figure 1. Molecular structure of **1**. Thermal ellipsoids are represented at 30% probability. All methyl hydrogen atoms have been omitted for clarity.

Table 1. Selected Bond Lengths (Å) and Angles (deg) for $Ru(NHC)_2(CO)_3$ (NHC = IEt_2Me_2 1, $I^iPr_2Me_2$ 2, I^iPr_2 3)

	1	2	3
Ru−C_{NHC}	2.142(2)	2.178(2) (ax)	2.153(2) (ax)
	2.133(2)	2.2019(17) (eq)	2.177(2) (eq)
Ru−CO	1.905(3)	1.880(2) (ax)	1.888(2) (ax)
	1.916(3)	1.8851(15) (eq)	1.884(2) (eq)
	1.915(3)	1.9055(18) (eq)	1.916(2) (eq)
C−O	1.150(4)	1.150(3) (ax)	1.155(3) (ax)
	1.158(3)	1.1634(19) (eq)	1.171(3) (eq)
	1.155(3)	1.16192) (eq)	1.152(3) (eq)
C_{NHC}−Ru−C_{NHC}	172.24(9)	88.52(7)	87.55(8)
OC−Ru−OC	103.64(14)	120.57(8)	128.07(9)
	124.34(13)	91.80(11)	92.31(10)
	131.98(13)	87.00(9)	88.17(10)

in **1** (2.133(2), 2.142(2) Å). In all three of the structures, one of the three Ru−C−O angles is close to linear (in the cases of **2** and **3**, it is the carbonyl ligand trans to NHC), while the other two are noticeably bent, the largest deviations being observed for **2** (Ru(1)−C(1)−O(1) 174.55(16)°, Ru(1)−C(2)−O(2) 167.24(19)°). As in the structure of **1**, there is a modicum of NHC tilting observed in **2** and **3**. This feature is reflected in the N−$C_{carbene}$−Ru angles for both compounds, where the degree of tilt corresponds directly to widened angles in the equatorial plane containing the metal, which thereby facilitates increased proximity for one pendant α-hydrogen in each carbene to the ruthenium center (for **2**: N(2)−C(4)−Ru(1), 126.57(15); N(1)−C(4)−Ru(1), 129.19(15); N(4)−C(15)−Ru(1), 129.67(12); N(3)−C(15)−Ru(1), 126.57(12)°. For **3**: N(2)−C(4)−Ru(1), 126.36(16); N(1)−C(4)−Ru(1), 130.09(15); N(4)−C(13)−Ru(1), 129.11(15); N(3)−C(13)−Ru(1), 127.58(15)°). The impact of methyl substitution on the backbone carbons of the imidazolylidene ring appears to have a minimal effect on the relative twist of the cis ligands with angles of 67.5° and 67.2° between the least-squares NHC ring planes in **2** and **3**, respectively.

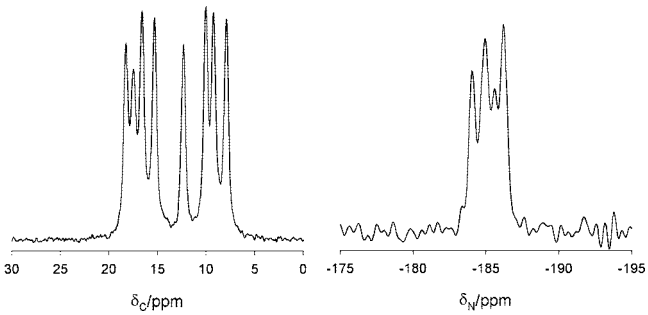

Figure 2. Solid-state NMR spectra of **1** at 206 K. Methyl region of ^{13}C spectrum (left) and ^{15}N spectrum (right).

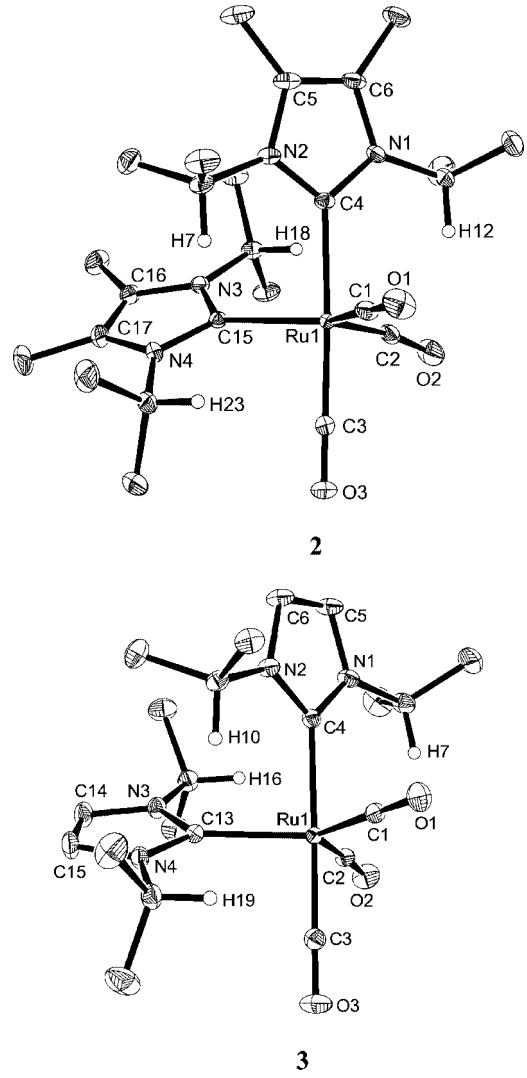

Figure 3. Molecular structures of **2** and **3**. Thermal ellipsoids are represented at 30% probability. Solvent (in **3**), NHC backbone hydrogens and all methyl hydrogen atoms have been omitted for clarity.

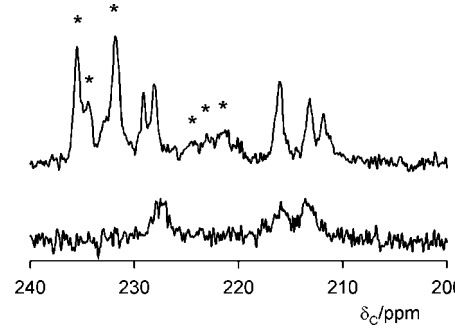

Figure 4. Carbonyl region of the solid-state ^{13}C NMR spectra of **3** at (bottom) 303 K and (top) 206 K (* = spinning sideband).

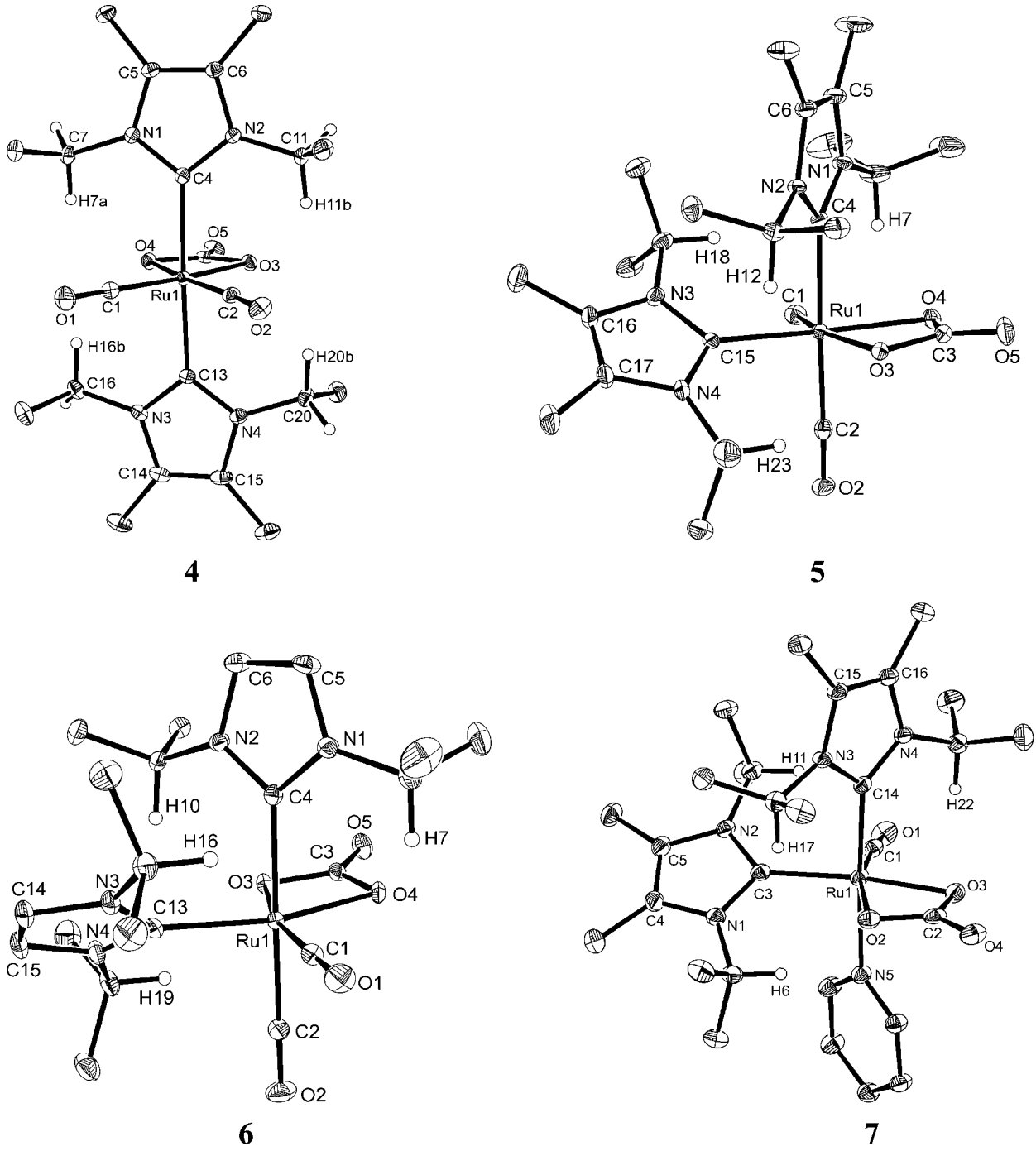

Figure 5. Molecular structures of the carbonato complexes **4**–**7** (only molecule based on Ru1 is shown for **4**). Thermal ellipsoids are represented at 30% probability. Solvent (in **4**, **6**, and **7**), NHC backbone hydrogens, and all methyl hydrogen atoms have been omitted for clarity.

^{13}C and ^{15}N solid-state NMR spectra of **3** were also recorded at 303 and 206 K. While the general forms of the spectra are similar to those for **1**, there are a number of different features, the most notable being that the $Ru-C_{NHC}$ resonances are quite well separated (δ 184 and δ 181), consistent with two very different carbene environments. At ambient temperature, the carbonyl signals were rather broad and indistinct but sharpened upon cooling to give more than three signals, as apparent in the spectrum at 206 K shown in Figure 4. This behavior is consistent with a dynamic system.

IR Spectroscopy of 1–3. The IR spectrum of **1** recorded in KBr (see below for issues associated with making samples in KBr), Nujol, or C_6D_6 displayed, in each case, a broadband centered at ca. 1833 cm^{-1}, along with a much weaker feature at 1931 cm^{-1}.[16] The presence of more than one CO band in both *trans*-$Ru(NHC)_2(CO)_3$ (NHC = IMes, ICy) and *trans*-$Ru(IMes)(PPh_3)(CO)_3$ has been noted previously.[11–13] The spectrum of **2** (in nujol or KBr) contained a structured low frequency band, with components at 1830, 1839, 1854, and 1860 cm^{-1}, plus an equally intense higher frequency absorption at 1955 cm^{-1} (these bands shifted in C_6D_6 solution to 1836 (sh), 1845 (vs), 1867 (s), and 1967 (s) cm^{-1}). On the basis of their C_s symmetry, **2** and **3** would be expected to show three carbonyl

(16) Li, C.; Olivan, M.; Nolan, S. P.; Caulton, K. G. *Organometallics* **1997**, *16*, 4223–4225.

Table 2. Selected Bond Lengths (Å) and Angles (deg) for $Ru(NHC)_2(CO)_2(CO_3)$ (NHC = IEt_2Me_2 4, $I^iPr_2Me_2$ 5, I^iPr_2 6) and $Ru(I^iPr_2Me_2)_2(CO)(C_5H_5N)(CO_3)$ (7)

	4	5	6	7
$Ru-C_{NHC}$	2.1290(18)	2.151(3) (ax)	2.121(3) (ax)	2.066(2) (ax)
	2.1318(17)	2.109(2) (eq)	2.083(3) (eq)	2.081(2) (eq)
Ru−CO	1.8606(19)	1.901(4) (ax)	1.937(3) (ax)	1.820(3) (eq)
	1.8681(19)	1.845(2) (eq)	1.861(3) (eq)	
Ru−O	2.1045(12)	2.0975(13)[a]	2.0992(19)[a]	2.1211(16)[a]
	2.0945(12)	2.1003(12)[b]	2.1165(19)[b]	2.1132(16)[b]
Ru−N				2.174(2)
$C_{NHC}-Ru-C_{NHC}$	172.94(6)[c]	88.76(10)	89.21(11)	92.47(9)
	170.37(3)[d]			
OC−Ru−CO	83.59(8)[c]	86.01(13)	88.90(13)	
	84.82(9)[d]			

[a] Trans to CO. [b] Trans to NHC. [c] Molecule based on Ru1. [d] Molecule based on Ru2.

absorptions, as seen for seen for $M(P-P)(CO)_3$ (M = Fe, Ru; P−P = chelating phosphine),[17] in which there is an axial–equatorial arrangement of the phosphine ligands. This may explain the structured low frequency IR band.

Variable-Temperature Solution NMR Studies of 1–3. The *N*-Et region of the ^1H NMR spectrum of **1** in toluene-d_8 solution at room temperature contained a quartet and triplet, consistent with all four ethyl groups being equivalent as a result of free rotation about both $Ru-C_{NHC}$ bonds.[18] Surprisingly, given the inequivalence of the NHCs in the solid-state structures of **2** and **3**, their ambient-temperature ^1H NMR spectra exhibited only a single ^{i}Pr doublet and septet in each case (the $^{13}C\{^1H\}$ spectrum of each compound displayed one Ru−NHC and one Ru−CO resonance) indicative of fluxional systems.[19] The fluxionality could not be frozen out even upon cooling to 195 K.[20]

Oxidation of $Ru(NHC)_2(CO)_3$ to the Carbonato Complexes $Ru(NHC)_2(CO)_2(CO_3)$. Complexes **2** and **3** proved to be susceptible to oxidation in air in the solid state to yield the carbonato complexes $Ru(NHC)_2(CO)_2(CO_3)$ ($I^iPr_2Me_2$ **5**, I^iPr **6**). Traces of **6** were apparent in the IR spectrum of **3** in KBr made up in air, with two ν_{CO} bands of comparable intensity at 2044 and 1954 cm^{-1}, and signals characteristic of a bidentate carbonato ligand at 1586 and 1211 cm^{-1}.[21] Complete conversion to **6** necessitated leaving a solid sample of **3** in air for about a week, during which time the material changed color from red-orange to dark black. However, only very low yields of product could be isolated using this route, suggesting (not surprisingly!) that much of the black color arises from the formation of overoxidized species. A more reliable path to both **5** and **6** involved subjecting pyridine-d_5[22] solutions of **2** and **3** to 1 atm of O_2 for very short periods of time (ca. 30 s) before complete removal of gas and solvent; prolonged oxygen exposure in solution produced a number of other unidentified (presumably oxidation) products.

The ^1H NMR spectrum of **6** (CD_2Cl_2, 298 K) displayed a sharp and a broad set of carbene resonances, which upon cooling to 262 K resolved into a series of sharp resonances, with four different backbone CH and isopropyl methine groups and eight different ^{i}Pr methyl signals (see the Supporting Information for spectra). The high frequency region of the $^{13}C\{^1H\}$ PENDANT spectrum of **6** consisted of two carbene (δ 176.5, 169.0) and two carbonyl resonances (δ 201.3, 192.9) along with a signal at δ 166.8 for the carbonato carbon.

A second, minor product was identified in the oxidation reaction of **2** in pyridine in the form of $Ru(I^iPr_2Me_2)_2(CO)(C_5H_5N)(CO_3)$, **7**, resulting from the displacement of one of the CO ligands by the coordinating solvent. The X-ray crystal structures of **5**−**7** are shown in Figure 5, with salient bond lengths and angles reported in Table 2. All three structures show a distorted octahedral geometry at ruthenium and display the expected *cis*-carbene geometry. The Ru−axial ligand distances in both **5** and **6** are significantly longer than their equatorial counterparts (e.g., in **6**: Ru−NHC, 2.121(3) vs 2.083(3) Å; Ru−CO, 1.937(3) vs 1.861(3) Å). The Ru−NHC distances decrease in the order **5** > **6** > **7**, while the Ru−CO distances are longer in **6** than in **5**. All of the Ru−O distances are comparable to those in structurally characterized $Ru-CO_3$ complexes found in the literature.[23] As for **1**–**3**, there also is some inclination of the carbene ligand in the carbonato complexes (for **5**: N(2)−C(4)−Ru(1), 128.46(19); N(1)−C(4)−Ru(1), 126.95(19); N(4)−C(15)−Ru(1), 126.69(15); N(3)−C(15)−Ru(1), 127.68(17). **6**: N(1)−C(4)−Ru(1), 128.2(2); N(2)−C(4)−Ru(1), 127.2(2); N(4)−C(13)−Ru(1), 125.8(2); N(3)−C(13)−Ru(1), 129.7(2)°. **7**: N(3)−C(14)−Ru(1), 127.33(17); N(4)−C(14)−Ru(1), 128.10(16); N(1)−C(3)−Ru(1), 125.27(17); N(2)−C(3)−Ru(1), 130.56(18)°). Overall, replacement of two carbonyl ligands by one carbonate is concomitant with a minimal reduction on relative twist of the NHC ligands, with angles of 64.1° and 66.1° between the least-squares NHC ring planes in **5** and **6**, respectively. However, the comparative twist observed in **7** is substantially larger at 70.7°.

(17) (a) Manuel, T. A. *Inorg. Chem.* **1963**, *2*, 854–858. (b) Akhtar, M.; Ellis, P. D.; MacDiarmid, A. G.; Odom, J. D. *Inorg. Chem.* **1972**, *11*, 2917–2921. (c) Battaglia, L. P.; Delledonne, D.; Nardelli, M.; Pelizzi, C.; Predieri, G.; Chiusoli, G. P. *J. Organomet. Chem.* **1987**, *330*, 101–113. (d) Brookhart, M.; Chandler, W. A.; Pfister, A. C.; Santini, C. C.; White, P. S. *Organometallics* **1992**, *11*, 1263–1274. (e) Whittlesey, M. K.; Perutz, R. N.; Virrels, I. G.; George, M. W. *Organometallics* **1997**, *16*, 268–274.

(18) The VT proton spectrum of **1** in d_8-toluene-d_8 between 298 and 206 K showed only an ever-increasing broadening of the NCH_2 signal. The NCH_2CH_3 methyl resonance broadened (down to ca. 240 K) before sharpening again at 216 K.

(19) Warming toluene samples of **2** and **3** above 323 K resulted in gradual decomposition of the samples (see ref 15), preventing high-temperature NMR data from being recorded.

(20) See the Supporting Information for VT NMR spectra of **1**–**3** in other solvents.

(21) For other reports describing the oxidation of Ru/Os mono- and dicarbonyl complexes, see: (a) Laing, K. R.; Roper, W. R. *J. Chem. Soc., Chem. Commun.* **1968**, 1568–1569. (b) Siegl, W. O.; Lapporte, S. J.; Collman, J. P. *Inorg. Chem.* **1973**, *12*, 674–677. (c) Letts, J. B.; Mazanec, T. J.; Meek, D. W. *Organometallics* **1983**, *2*, 695–704. (d) Ogasawara, M.; Maseras, F.; Gallego-Planas, N.; Kawamura, K.; Ito, K.; Toyota, K.; Streib, W. E.; Komiya, S.; Eisenstein, O.; Caulton, K. G. *Organometallics* **1997**, *16*, 1979–1993.

(22) This was the only solvent that allowed dissolution of both the starting tricarbonyl complexes (which reacted with CD_2Cl_2) and carbonato products (which showed limited solubility in THF).

(23) (a) Belli Dell'Amico, D.; Calderazzo, F.; Labella, L.; Marchetti, F. *J. Organomet. Chem.* **2000**, *596*, 144–151. (b) Demerseman, B.; Mbaye, N. D.; Sémeril, D.; Toupet, L.; Bruneau, C.; Dixneuf, P. H. *Eur. J. Inorg. Chem.* **2006**, 1174–1181.

Synthesis of the *N*-ethyl carbonato complex $Ru(IEt_2Me_2)_2(CO)_2(CO_3)$ (**4**) proved to be less straightforward.[24] Reaction with O_2 in solution proved to be hard to control, while only about a 10% yield of product could be isolated when a solid sample of **1** was left to stand in air for three weeks. The cleanest route to **4** involved heating microcrystalline **1** under O_2 at 343 K overnight. The observation of one Ru−CO, one Ru−C_{NHC} resonance, and a single set of ethyl signals in the ^{13}C NMR spectrum indicated that the trans carbene arrangement from **1** is retained in **4** (Scheme 3). This was confirmed by an X-ray crystal structure determination (Figure 5). As shown in Table 2, the bond lengths and angles are unexceptional. However, the relative twist of the *trans*-carbene ligands varies considerably compared to that observed in **1**. In particular, the angles between the NHC rings based on the molecules containing Ru1 and Ru2 (see details on X-ray crystallography in the Experimental Section) are 23.1° and 6.8°, respectively. This difference may reflect, in part, the different conformations of the β-ethyl carbons in both molecules. In the latter molecule all four point in the same direction as the carbonyl ligands. This has the effect of sterically compressing the C_{NHC}−Ru−C_{NHC} angle subtended at Ru2 (170.37(7)°) relative to that the corresponding angle at Ru1 (172.94(6)°), where one pair of the β-ethyl carbons is staggered relative to the C_{NHC}−Ru−C_{NHC} vector.

Efforts to detect intermediate species en route to the carbonato compounds proved to be uninformative.[25] Thus, subjecting a sample of **1** to 1 atm of O_2 at 196 K showed only proton NMR signals attributable to the starting material all the way up to 273 K. Above this temperature, **1** rapidly converted to **4**.

Concluding Remarks

Three mononuclear N-heterocyclic carbene complexes $Ru(NHC)_2(CO)_3$ have been isolated from the room-temperature reactions of $Ru_3(CO)_{12}$ with the *N*-alkyl-substituted NHCs IEt_2Me_2, $I^iPr_2Me_2$, and I^iPr_2 and characterized by a combination of X-ray diffraction, solid-state, and solution NMR spectroscopy. Surprisingly, in the solid-state, the two *N*-^{i}Pr carbene products contain a cis-arrangement of the donor ligands, contrary to what is usually found for zerovalent group 8 $ML_2(CO)_3$ compounds. For a series of $ML(CO)_4$ complexes (L = PR_3, AsR_3, SbR_3), Einstein and Pomeroy showed that an equilibrium between axial and equatorial L isomers was related to both steric and electronic properties of L.[26] Given that all the NHCs in our study are extremely good σ-donors[27] and that what appears to be the least sterically obtrusive of the ligands (IEt_2Me_2) yields the "expected" trans isomer **1**, both sterics and electronics must play a role in determining the structures of **1**−**3**. All three tricarbonyl complexes can be oxidized to the dicarbonyl carbonato complexes in the solid-state and in solution, with the trans or cis arrangement of the NHC ligands being maintained. Further studies to establish conditions under which NHC incorporation into a cluster occurs (as in Schemes 1 and 2) versus the type of cluster fragmentation described here are in progress.

(24) It is worth noting that the formation of $Ru(PPh_3)_2(CO)_2(CO_3)$ by oxidation of $Ru(PPh_3)_2(CO)_3$ has been shown to be very slow in the solid state and to fail altogether in solution. Valentine, J.; Valentine, D., Jr.; Collman, J. P *Inorg. Chem.* **1971**, *10*, 219–225.

(25) (a) Curtis, M. D.; Han, K. R. *Inorg. Chem.* **1985**, *24*, 378–382. (b) Roper, W. R. *J. Organomet. Chem.* **1986**, *300*, 167–190. (c) See also ref 21d.

(26) Martin, L. R.; Einstein, F. W. B.; Pomeroy, R. K. *Inorg. Chem.* **1985**, *24*, 2777–2785.

(27) For a theoretical prediction of carbene basicity, see: Magill, A. M.; Cavell, K. J.; Yates, B. F *J. Am. Chem. Soc.* **2004**, *126*, 8717–8724.

Experimental Section

General Comments. All manipulations were carried out using standard Schlenk or glovebox techniques under an atmosphere of argon. Solvents were purified using an MBraun SPS solvent system (Et_2O, CH_2Cl_2), Innovative Technologies solvent system (THF, hexane), or under a nitrogen atmosphere from sodium benzophenone ketyl (benzene, toluene) or Mg/I_2 (EtOH). Deuterated solvents (Fluorochem) were dried over molecular sieves (pyridine-d_5) or vacuum transferred from potassium (thf-d_8, toluene-d_8, C_6D_6) or CaH_2 (CD_2Cl_2). IEt_2Me_2, $I^iPr_2Me_2$, and I^iPr_2 were prepared according to a literature method.[28]

Solution NMR spectra were recorded in Bath on Bruker Avance 400 and 500 NMR spectrometers, at 298 K unless otherwise stated, and referenced as follows: toluene (^1H, δ 2.09; $^{13}C\{^1H\}$, δ 21.3), THF (δ 3.58; δ 67.2), dichloromethane (δ 5.32; δ 53.7), and pyridine (δ 8.72; δ 123.5). $^1H-^{13}C\{^1H\}$ HMQC/HMBC experiments were performed using standard Bruker pulse sequences. Solid-state NMR spectra were recorded in Durham under nitrogen on a Varian VNMRS 400 MHz spectrometer (6.0 mm MAS probe) at 303 and 206 K (actual sample temperatures). Temperature calibration was carried out using MeOH, and then lead nitrate at sample spin rates appropriate to the measurements reported here. The following acquisition parameters were used: **1**, ^{13}C: recycle time 6.0 s (at 303 K; 2s at 206 K), contact time 1.00 ms, spin rate 6.80 kHz; ^{15}N: recycle time as for carbon, contact time 10.00 ms, spin rate 6.80 kHz. **3**, ^{13}C: recycle time 1.5 s (at 303 K; 1s at 206 K), contact time 10.00 ms, spin rate 6.80 kHz (at 303 K; 5.20 kHz at 206 K); ^{15}N: recycle time as for carbon, contact time 10.00 ms, spin rate 5.20 kHz. Chemical shifts were referenced to TMS (^{13}C) by setting the high-frequency signal for adamantane to 38.4 ppm and to nitromethane (^{15}N) by setting the nitrate signal from solid ammonium nitrate to −5.1 ppm.

IR spectra were recorded on a Nicolet Nexus FTIR spectrometer. Elemental analyses were performed by Elemental Microanalysis Ltd., Okehampton, Devon, UK. Mass spectra were recorded using a micrOTOF electrospray time-of-flight (ESI-TOF) mass spectrometer (Bruker Daltonik GmbH) coupled to an Agilent 1200 LC system (Agilent Technologies).

$Ru(IEt_2Me_2)_2(CO)_3$ (1). IEt_2Me_2 (100 mg, 0.66 mmol) was added to a THF (10 mL) solution of $Ru_3(CO)_{12}$ (70 mg, 0.11 mmol) and vigorous bubbling of the solution observed straight away. Removal of the solvent afforded an orange-red microcrystalline solid, which was washed with hexane (3 × 5 mL) and then recrystallized from THF−hexane. Yield: 135 mg (83%). ^1H HMR (500 MHz, THF-d_8, 298K): δ 4.43 (q, J_{HH} = 7.2 Hz, 8H, CH_2CH$_3$), 2.17 (s, 12H, NCCH_3), 1.22 (t, J_{HH} = 7.2 Hz, 12H, CH$_2$CH_3). $^{13}C\{^1H\}$ NMR (THF-d_8, 298K): δ 218.6 (s, *C*O), 181.6 (s, N*C*N), 125.6 (s, N*C*CH$_3$), 44.8 (s, *C*H$_2$CH$_3$), 15.7 (s, NC*C*H$_3$), 9.5 (s, CH$_2$*C*H$_3$). IR (C_6D_6, cm^{-1}): 1967 w, 1937 w, 1849 sh, 1836 vs, all ν_{CO}. Anal. Found (calcd) for $C_{21}H_{32}N_4O_3Ru$: C, 51.43 (51.52); H, 6.63 (6.59); N, 11.19 (11.44).

$Ru(I^iPr_2Me_2)_2(CO)_3$ (2). The same procedure as for **1** was used with $I^iPr_2Me_2$ (120 mg, 0.66 mmol) and $Ru_3(CO)_{12}$ (70 mg, 0.11 mmol). Yield: 148 mg (82%). ^1H NMR (500 MHz, THF-d_8, 298 K): δ 5.99 (sept, J_{HH} = 7.2 Hz, 4H, C*H*(CH$_3$)$_2$), 2.23 (s, 12H, NCCH_3), 1.26 (d, J_{HH} = 7.2 Hz, 24H, CH(CH_3)$_2$). $^{13}C\{^1H\}$ NMR (THF-d_8, 298 K): δ 217.7 (s, *C*O), 187.3 (s, N*C*N), 126.4 (s, N*C*CH$_3$), 55.0 (s, *C*H(CH$_3$)$_2$), 21.3 (s, NCH(*C*H$_3$)$_2$), 10.7 (s, NC*C*H$_3$). IR (C_6D_6, cm^{-1}): 1967 s, 1867 s, 1845 vs, 1836 sh, all ν_{CO}. Anal. Found (calcd) for $C_{25}H_{40}N_4O_3Ru$: C, 54.39 (55.05); H, 7.13 (7.39); N, 9.99 (10.27).

$Ru(I^iPr_2)_2(CO)_3$ (3). The same procedure as for **1** was used with I^iPr_2 (100 mg, 0.66 mmol) and $Ru_3(CO)_{12}$ (70 mg, 0.11 mmol). Yield: 154 mg (95%). ^1H NMR (500 MHz, THF-d_8, 298K): δ 7.24 (s, 4H, NC*H*), 5.57 (sept, J_{HH} = 7.0 Hz, 4H, C*H*(CH$_3$)$_2$), 1.26 (d,

(28) Kühn, N.; Kratz, T. *Synthesis* **1993**, 561–563.

Table 3. Crystal Data and Structure Refinement for Compounds 1−7

compd	**1**	**2**	**3**	**4**	**5**	**6**	**7**
empirical formula	$C_{21}H_{32}N_4O_3Ru$	$C_{25}H_{40}N_4O_3Ru$	$C_{25}H_{40}N_4O_4Ru$	$C_{44}H_{70}Cl_4N_8O_{11}Ru_2$	$C_{25}H_{40}N_4O_5Ru$	$C_{22}H_{34}Cl_2N_4O_5Ru$	$C_{33}H_{53}N_5O_5Ru$
formula weight	489.58	545.68	561.68	1231.02	577.68	606.50	700.87
crystal system	Orthorhombic	Monoclinic	Monoclinic	Monoclinic	Monoclinic	Monoclinic	Monoclinic
space group	*Pbca*	$P2_1$	$P2_1/a$	$P2/c$	$P2_1$	$P2_1/n$	$P2_1/c$
a/Å	9.2580(1)	10.6340(1)	16.5190(2)	15.6640(1)	10.6020(2)	10.2360(1)	11.3900(2)
b/Å	16.6670(2)	12.0530(2)	10.7430(2)	9.6590(1)	12.0620(2)	10.7810(1)	18.2000(2)
c/Å	29.1940(3)	11.2800(2)	17.3800(2)	36.0120(3)	11.3930(2)	25.1870(3)	16.4380(2)
α/deg	90.0	90.0	90.0	90.0	90.0	90.0	90.0
β/deg	90.0	110.466(1)	114.699(1)	93.325(1)	110.069(1)	92.132(1)	98.313(1)
γ/deg	90.0	90.0	90.0	90.0	90.0	90.0	90.0
U/Å^3	4504.72(9)	1354.52(4)	2802.15(7)	5439.39(8)	1368.49(4)	2777.57(5)	3371.76(8)
Z	8	2	4	4	2	4	4
D_c/g cm^{-3}	1.444	1.338	1.331	1.503	1.402	1.450	1.381
μ/ mm^{-1}	0.724	0.610	0.594	0.813	0.613	0.794	0.512
F(000)	2032	572	1176	2536	604	1248	1480
crystal size/mm	0.35 × 0.30 × 0.30	0.50 × 0.35 × 0.25	0.40 × 0.20 × 0.20	0.30 × 0.25 × 0.13	0.25 × 0.20 × 0.20	0.20 × 0.12 × 0.07	0.15 × 0.12 × 0.10
$\theta_{min,max}$ for data collection	3.57, 30.02	3.68, 30.13	3.79, 30.04	3.53, 30.07	3.65, 27.48	3.62, 27.54	3.58, 27.51
index ranges	$-13 \le h \le +13$; $-23 \le k \le +23$; $-41 \le l \le +41$	$-14 \le h \le +14$; $-16 \le k \le +16$; $-15 \le l \le +15$	$-23 \le h \le +23$; $-15 \le k \le +14$; $-18 \le l \le +24$	$-22 \le h \le +22$; $-13 \le k \le +13$; $-50 \le l \le +50$	$-13 \le h \le +13$; $-15 \le k \le +15$; $-14 \le l \le +14$	$-13 \le h \le +13$; $-13 \le k \le +13$; $-32 \le l \le +32$	$-14 \le h \le +14$; $-23 \le k \le +23$; $-21 \le l \le +21$
reflections collected	61789	27748	53080	94858	26125	40649	65325
independent reflections, R_{int}	6559, 0.0778	7894, 0.0377	8170, 0.0657	15843, 0.0541	6230, 0.0360	6352, 0.0348	7717, 0.0617
reflections observed (>2σ)	4295	7311	5851	12505	5837	5763	6024
max, min transmission	0.82, 0.75	0.71, 0.67	0.84, 0.80	0.85, 0.76	0.94, 0.91	0.82, 0.78	0.90, 0.88
data/restraints/parameters	6559/0/267	7894/1/311	8170/66/362	15843/2/638	6230/1/328	6352/0/325	7717/0/409
goodness-f-fit n F^2	1.031	1.058	1.037	1.028	1.079	1.174	1.046
final *R*1, *wR*2 [$I > 2\sigma(I)$]	0.0386, 0.0840	0.0254, 0.0533	0.0369, 0.0777	0.0313, 0.0698	0.0249, 0.0544	0.0390, 0.0870	0.0371, 0.0819
final *R*1, *wR*2 (all data)	0.0763, 0.0980	0.0304, 0.0551	0.0692, 0.0895	0.0496, 0.0764	0.0291, 0.0560	0.0447, 0.0895	0.0563, 0.0899
largest diff peak, hole/e Å^{-3}	1.445, −0.791	1.028, −0.701	1.661, −0.901	0.707, −0.842	0.741, −0.626	1.455, −1.491	0.723, −0.639
absolute structure parameter		−0.036(18)			−0.027(18)		

J_{HH} = 7.0 Hz, 24H, CH(CH_3)$_2$). ^{13}C{^{1}H}NMR (THF-d_8, 298K): δ 217.8 (s, *C*O), 184.4 (s, N*C*N), 118.2 (s, H*C*=*C*H), 53.2 (s, *C*H(CH$_3$)$_2$), 23.1 (s, CH(*C*H$_3$)$_2$). IR (C_6D_6, cm^{-1}): 1970 m, 1852 sh, 1841 vs, all ν_{CO}. Anal. Found (calcd) for $C_{21}H_{32}N_4O_3Ru$: C, 51.57 (51.52); H, 6.65 (6.59); N, 11.10 (11.44).

Ru(IEt$_2$Me$_2$)$_2$(CO)$_2$(CO$_3$) (4). A solid sample of Ru(IEt$_2$Me$_2$)$_2$(CO)$_3$ (100 mg, 0.20 mmol) was heated for 14 h at 70 °C in an ampule fitted with a J. Youngs PFTE tap under 1 atm O_2. The resulting carbonato complex Ru(IEt$_2$Me$_2$)$_2$(CO)$_2$(CO$_3$) was extracted with THF (3 × 5 mL), pumped to dryness, and then washed with hexane (3 × 5 mL) to leave a light brown solid. Yield: 50 mg (48%). Crystals for X-ray diffraction were grown from CH_2Cl_2/hexane. ^{1}H NMR (500 MHz, THF-d_8, 298K): δ 4.37 (q, J_{HH} = 7.0 Hz, 8H, CH_2CH$_3$), 2.20 (s, 12H, NCCH_3), 1.44 (t, J_{HH} = 7.0 Hz, 12H, CH$_2$CH_3). ^{13}C{^{1}H} NMR (THF-d_8, 298K): δ 201.9 (s, *C*O), 174.5 (s, N*C*N), 164.4 (s, *C*O$_3$), 126.0 (s, N*C*CH$_3$), 43.6 (s, *C*H$_2$CH$_3$), 16.8 (s, NC*C*H$_3$), 8.8 (s, CH$_2$*C*H$_3$). IR (KBr, cm^{-1}): 2024 ν_{CO}, 1947 ν_{CO}, 1612 ν, 1250 ν_{CO}. ESI-TOF MS: [M+Na]$^+$ m/z = 545.1300 (theoretical m/z = 545.1314). Anal. Found (calcd) for $C_{21}H_{32}N_4O_5Ru \cdot H_2O$: C, 47.05 (46.74); H, 6.31 (6.35); N, 10.17 (10.38). The molecule of water came from exposure of sample to air, and appeared in the IR spectrum as a broad O–H stretch at 3423 cm^{-1}.

Ru(I^{i}Pr$_2$Me$_2$)$_2$(CO)$_2$(CO$_3$) (5) and Ru(I^{i}Pr$_2$Me$_2$)$_2$(CO)(C$_5$H$_5$N)(CO$_3$) (7). Ru(I^{i}Pr$_2$Me$_2$)$_2$(CO)$_3$ (150 mg, 0.28 mmol) was dissolved in pyridine (2 mL) in an ampule fitted with a J. Young's resealable PTFE valve, freeze–pump–thaw degassed, and then placed under 1 atm O_2. After shaking for 30 s, the gas and solvent were removed under vacuum. The residue was washed with THF (2 × 3 mL) to give **5** as a pale yellow solid. Yield: 95 mg (60%). ^{1}H NMR (400 MHz, CD_2Cl_2, 298 K): δ 5.95 (sept, J_{HH} = 7.0 Hz, 1H, C*H*(CH$_3$)$_2$), 5.71 (sept, J_{HH} = 7.0 Hz, 1H, C*H*(CH$_3$)$_2$), 4.80 (sept, J_{HH} = 7.0 Hz, 1H, C*H*(CH$_3$)$_2$), 4.67 (sept, J_{HH} = 7.0 Hz, 1H, C*H*(CH$_3$)$_2$), 2.31 (s, 3H, NCCH_3), 2.26 (s, 3H, NCCH_3), 2.19 (s, 3H, NCCH_3), 2.14 (s, 3H, NCH_3), 1.62 (d, J_{HH} = 7.0 Hz, 3H, CH(CH_3)), 1.60–158 (m, 6H, CH(CH_3)), 1.56 (d, J_{HH} = 7.0 Hz, 3H, CH(CH_3)), 1.33 (d, J_{HH} = 7.0 Hz, 3H, CH(CH_3)), 1.32 (d, J_{HH} = 6.9 Hz, 3H, CH(CH_3)), 0.85 (d, J_{HH} = 7.0 Hz, 3H, CH(CH_3)), 0.72 (d, J_{HH} = 6.9 Hz, 3H, CH(CH_3)). ^{13}C{^{1}H} NMR (CD_2Cl_2, 298 K): δ 200.9 (s, *C*O), 193.1 (s, *C*O), 177.5 (s, N*C*N), 168.8 (s, N*C*N), 166.7 (*C*O$_3$), 128.0 (s, H$_3$C*C*=*C*CH$_3$), 127.1 (s, H$_3$C*C*=*C*CH$_3$), 126.4 (s, N*C*CH$_3$), 126.1 (s, N*C*CH$_3$), 54.0 (s, *C*H(CH$_3$)$_2$), 53.7 (s, *C*H(CH$_3$)$_2$), 52.8 (s, *C*H(CH$_3$)$_2$), 52.6 (s, *C*H(CH$_3$)$_2$), 23.7 (s, NCH(*C*H$_3$)$_2$), 22.7 (s, NCH(*C*H$_3$)$_2$), 22.5 (s, NCH(*C*H$_3$)$_2$), 22.2 (s, NCH(*C*H$_3$)$_2$), 21.9 (s, NCH(*C*H$_3$)$_2$), 21.5 (s, NCH(*C*H$_3$)$_2$), 19.7 (s, NCH(*C*H$_3$)$_2$), 19.5 (s, NCH(*C*H$_3$)$_2$), 10.8 (s, NC*C*H$_3$), 10.7 (s, NC*C*H$_3$), 10.6 (s, NC*C*H$_3$). IR (KBr, cm^{-1}): 2034 ν_{CO}, 1945 ν_{CO}, 1593 ν_{CO}. ESI-TOF MS: [M − CO + H]$^+$ m/z = 551.2152 (theoretical m/z = 551.2172).

Ru(I^{i}Pr$_2$Me$_2$)$_2$(CO)(C$_5$H$_5$N)(CO$_3$) (**7**) was isolated in 17% yield (30 mg) from the same reaction upon crystallization of the THF washings. ^{1}H NMR (500 MHz, pyridine-d_5, 298 K): δ 6.52 (sept, 1H, J_{HH} = 7.00 Hz, C*H*(CH$_3$)$_2$), 5.85 (sept, 1H, J_{HH} = 7.00 Hz, C*H*(CH$_3$)$_2$), 5.42 (sept, 1H, J_{HH} = 7.00 Hz, C*H*(CH$_3$)$_2$), 5.23 (sept, 1H, J_{HH} = 7.00 Hz, C*H*(CH$_3$)$_2$), 2.15 (s, 3H, NCCH_3), 2.08 (s, 3H, NCCH_3), 2.05 (s, 3H, NCCH_3), 1.99 (s, 3H, NCCH_3), 1.65 (d, 3H, J_{HH} = 7.00 Hz, CH(CH_3)$_2$), 1.62–1.60 (m, 6H, CH(CH_3)$_2$), 1.49 (d, 3H, J_{HH} = 7.00 Hz, CH(CH_3)$_2$), 1.45 (d, 3H, J_{HH} = 7.00 Hz, CH(CH_3)$_2$), 0.88 (d, 3H, J_{HH} = 7.00 Hz, CH(CH_3)$_2$), 0.76 (d, 3H, J_{HH} = 7.00 Hz, CH(CH_3)$_2$), 0.46 (d, 3H, J_{HH} = 7.00 Hz, CH(CH_3)$_2$). ^{13}C{^{1}H} (pyridine-d_5, 298 K): δ 208.9 (s, *C*O), 180.9 (s, N*C*N), 178.1 (s, N*C*N), 169.4 (*C*O$_3$), 127.2 (s, N*C*CH$_3$), 126.4 (s, N*C*CH$_3$), 126.1 (s, N*C*CH$_3$), 126.0 (s, N*C*CH$_3$), 53.3 (s, *C*H(CH$_3$)$_2$), 52.8 (s, *C*H(CH$_3$)$_2$), 52.2 (s, *C*H(CH$_3$)$_2$), 50.6 (s, *C*H(CH$_3$)$_2$), 24.1 (s, CH(*C*H$_3$)$_2$), 23.2 [s, CH(*C*H$_3$)$_2$), 23.1 (s, CH(*C*H$_3$)$_2$), 22.2 (s, CH(*C*H$_3$)$_2$), 21.6 (s, CH(*C*H$_3$)$_2$), 21.0 (s, CH(*C*H$_3$)$_2$), 19.8 (s, CH(*C*H$_3$)$_2$), 19.6 (s, CH(*C*H$_3$)$_2$), 10.5 (s, NC*C*H$_3$), 10.4 (s, NC*C*H$_3$), 10.3 (s, NC*C*H$_3$). Spectra were also recorded in CD_2Cl_2 to allow the coordinated pyridine resonances to be observed. ^{1}H (500 MHz, CD_2Cl_2, 298 K): δ 8.51 (m, 2H, *o*-C*H* (pyr)), 7.70 (m, 1H, *p*-C*H* (pyr)), 7.30 (m, 2H, *m*-C*H* (pyr)), 5.98 (sept, 1H, J_{HH} = 7.00 Hz, C*H*(CH$_3$)$_2$), 5.43 (sept, 1H, J_{HH} = 7.00 Hz, C*H*(CH$_3$)$_2$), 5.06 (sept, 1H, J_{HH} = 7.00 Hz, C*H*(CH$_3$)$_2$), 5.00 (sept, 1H, J_{HH} = 7.00 Hz, C*H*(CH$_3$)$_2$), 2.25 (s, 3H, NCCH_3), 2.19 (s, 3H, NCCH_3), 2.17 (s, 3H, NCCH_3), 2.15 (s, 3H, NCCH_3), 1.62 (d, 3H, J_{HH} = 7.00 Hz, CH(CH_3)$_2$), 1.51–1.47 (m, 6H, CH(CH_3)$_2$), 1.43 (d, 3H, J_{HH} = 7.00 Hz, CH(CH_3)$_2$), 1.39 (d, 3H, J_{HH} = 7.00 Hz, CH(CH_3)$_2$), 0.87 (d, 3H, J_{HH} = 7.00 Hz, CH(CH_3)$_2$), 0.73 (d, 3H, J_{HH} = 7.00 Hz, CH(CH_3)$_2$), 0.44 (d, 3H, J_{HH} = 7.00 Hz, CH(CH_3)$_2$). ^{13}C{^{1}H} (CD_2Cl_2, 298 K): δ 208.3 (s, *C*O), 179.7 (s, N*C*N), 176.8 (s, N*C*N), 168.7 (*C*O$_3$), 153.0 (s, *ortho*-*C*H (pyr)), 137.2 (s, *para*-*C*H (pyr)), 127.4 (s, N*C*CH$_3$), 126.4 (s, N*C*CH$_3$), 126.2 (s, N*C*CH$_3$), 126.1 (s, N*C*CH$_3$), 125.2 (s, *meta*-*C*H (pyr)), 53.3 (s, *C*HCH$_3$), 52.8 (s, *C*HCH$_3$), 52.2 (s, *C*HCH$_3$), 50.8 (s, *C*HCH$_3$), 23.6 (s, CH*C*H$_3$), 23.1 (s, CH*C*H$_3$), 22.9 (s, CH*C*H$_3$), 22.1 (s, CH*C*H$_3$), 21.5 (s, CH*C*H$_3$), 20.8 (s, CH*C*H$_3$), 20.0 (s, CH*C*H$_3$), 19.6 (s, CH*C*H$_3$), 10.7 (s, NC*C*H$_3$), 10.6 (s, NC*C*H$_3$). IR (Nujol, cm^{-1}): 1905 ν_{CO}, 1643 ν_{OCO}. ESI-TOF MS: [M − C$_5$H$_5$N + H]$^+$ m/z = 551.2149 (theoretical m/z = 551.2172).

Ru(I^{i}Pr$_2$)$_2$(CO)$_2$(CO$_3$) (6). The same procedure as for **5** was used, reacting **3** (150 mg, 0.31 mmol) with O_2. Yield: 85 mg (43%). ^{1}H NMR (400 MHz, CD_2Cl_2, 298 K): δ 7.23 (d, J_{HH} = 2.40 Hz, 2H, NC*H*), 7.11 (br s, 1H, NC*H*), 7.05 (d, J_{HH} = 2.40 Hz, 1H, NC*H*), 6.96 (br s, 1H, NC*H*), 5.72 (sept, J_{HH} = 6.80 Hz, 1H, C*H*(CH$_3$)$_2$), 5.43 (br sept, 1H, C*H*(CH$_3$)$_2$), 4.43 (sept, J_{HH} = 6.80 Hz, 1H, C*H*(CH$_3$)$_2$), 4.37 (br sept, 1H, C*H*(CH$_3$)$_2$), 1.57 (br d, J_{HH} = 6.80 Hz, 3H, CH(CH_3)), 1.54–1.52 (m, 9H, CH(CH_3)), 1.32 (d, J_{HH} = 6.80 Hz, 3H, CH(CH_3)), 1.28 (br d, J_{HH} = 6.80 Hz, 3H, CH(CH_3)), 0.86 (d, J_{HH} = 6.80 Hz, 3H, CH(CH_3)), 0.72 (br d, J_{HH} = 6.9 Hz, 3H, CH(CH_3)). ^{13}C{^{1}H} NMR (CD_2Cl_2, 298 K): δ 201.3 (s, *C*O), 192.9 (s, *C*O), 176.5 (s, N*C*N), 169.0 (s, N*C*N), 166.8 (*C*O$_3$), 119.6 (s, N*C*H), 119.0 (s, N*C*H), 118.2 (s, N*C*H), 118.0 (s, N*C*H), 53.1 (s, N*C*H), 52.8 (s, N*C*H), 52.0 (s, N*C*H), 51.8 (s, N*C*H), 25.9 (s, CH*C*H$_3$), 24.8 (s, CH*C*H$_3$), 24.5 (s, CH*C*H$_3$), 24.3 (s, CH*C*H$_3$), 23.6 (s, CH*C*H$_3$), 23.5 (s, CH*C*H$_3$), 21.9 (s, CH*C*H$_3$), 21.6 (s, CH*C*H$_3$). IR (KBr, cm^{-1}): 2044 ν_{CO}, 1954 ν_{CO}, 1586 ν_{OCO}. ESI-TOF MS: [M − CO + H]$^+$ m/z = 495.1540 (theoretical m/z = 495.1545). Anal. Found (calcd) for $C_{21}H_{32}N_4O_5Ru$: C, 48.94 (48.36); H, 6.01 (6.18); N, 10.61 (10.74).

X-ray Crystallography. Single crystals of **1**–**7** were analyzed at 150(2) K using graphite-monochromated Mo Kα radiation and a Nonius Kappa CCD diffractometer. Data collection and refinement details are summarized in Table 3. The structures were solved using SHELXS-97 and refined using SHELXL-97.[29] Convergence was unremarkable throughout, except for the points of note below. In **3**, the asymmetric unit was seen to contain a disordered fragment of solvent, which was best modeled as one THF molecule at two close sites, in a 60:40 ratio. Solvent ADPs were restrained to be similar in the individual fragments, and the O−C distances were refined subject to being similar. The asymmetric unit in **4** comprises two bis-carbene ruthenium complex molecules, two molecules of dichloromethane, and one molecule of water. The hydrogen atoms in the latter are implicated in hydrogen bonding to carbonato oxygens, and as such, they were readily located in the penultimate difference Fourier map and subsequently refined at a distance of 0.9 Å from the parent oxygen, O11. This water oxygen interacts with H44A (in the solvent moiety containing Cl3), while both hydrogens in the solvent entity based on Cl1 are involved in interactions with carbonato oxygens in the molecule based on Ru1. One molecule of CH_2Cl_2 (in which one of the chlorines was

(29) Sheldrick, G. M. *Acta Crystallogr.* **1990**, 467–473, A46. Sheldrick, G. M, SHELXL-97, a computer program for crystal structure refinement, University of Göttingen, 1997.

disordered equally over two sites) was also found in the asymmetric unit of **6**, while in **7** there was evidence for one molecule of thf within the asymmetric unit.

Crystallographic data for **1**–**7** have been deposited with the Cambridge Crystallographic Data Centre as supplementary publications CCDC 659206 (**1**), 659208 (**2**), 659207 (**3**), 660512 (**4**), 659209 (**5**), 659210 (**6**) and 659211 (**7**). Copies of these data can be obtained free of charge on application to CCDC, 12 Union Road, Cambridge CB2 1EZ, UK [fax(+44) 1223 336033, e-mail: deposit@ccdc.cam.ac.uk].

Acknowledgment. We thank EPSRC for financial support (project studentship for O.S.) and the EPSRC solid-state NMR service for data collection. Dr. John Lowe is gratefully acknowledged for helpful NMR discussions.

Supporting Information Available: VT NMR data for **1**–**3** and **6**. X-ray crystallographic files (CIF) for complexes **1**−**7**. This material is available free of charge via the Internet at http://pubs.acs.org.

OM700915T